Computer Science Department

TECHNICAL REPORT

STABILITY OF HYPERBOLIC FINITE-DIFFERENCE MODELS WITH ONE OR TWO BOUNDARIES

BY

*Lloyd N. Trefethen

November 1983

Report # 97

NEW YORK UNIVERSITY

Department of Computer Science
Courant Institute of Mathematical Sciences
251 MERCER STREET, NEW YORK, N.Y. 10012

STABILITY OF HYPERBOLIC FINITE-DIFFERENCE MODELS WITH ONE OR TWO BOUNDARIES

BY

*Lloyd N. Trefethen

November 1983

Report # 97

[To appear in S. Osher (ed.), Proceedings of the 1983 AMS-SIAM Summer Session on Large-scale Computations in Fluid Mechanics, AMS Lectures in Applied Mathematics series.]

AMS(MOS)subject classification:66M10

*Supported by an NSF Mathematical Sciences Postdoctoral Fellowship and by the U.S. Department of Energy under Contract DE-AC02-76-ER03077-V

Abstract: The stability of finite difference models of hyperbolic partial differential equations depends on how numerical waves propagate and reflect at boundaries. This paper presents an extended numerical example illustrating the key points of this theory.

0. Introduction

In the numerical solution of hyperbolic partial differential equations by finite differences, stability is well known to be a critical issue. As a first step the difference model must satisfy the von Neumann condition – that is, the basic formula should admit no exponentially growing Fourier modes. For linear problems with smoothly varying coefficients and no boundaries, this is essentially the whole story, and in fact if one rules out algebraically as well as exponentially growing local Fourier modes, then stability is assured. Results of this kind are widely known and are discussed in the superb book by Richtmyer and Morton [9].

When boundaries are introduced, the stability problem becomes more subtle. Even here the literature is copious, and a dozen or more people have made substantial contributions, including Godunov and Ryabenkii, Strang, Osher [7], Kreiss, Gustafsson, Sundström, Tadmor, and Michelson. The best known paper in this area is the one by Gustafsson, Kreiss, and Sundström in 1972 [4], which presents what is now often referred to as the "GKS stability theory". The great strength of the GKS paper is that it establishes a necessary and sufficient stability condition for difference models of very general form – three-point or multipoint stencil in space, two-level or multilevel in time, explicit or implicit, dissipative or nondissipative. A difficulty with the paper is that it is very hard to read, and this has regrettably limited its influence. Fortunately, some more accessible accounts have appeared recently, including the report by Gustafsson in this volume.

My own work in this field has been concerned with giving the stability question for initial boundary value problem models a physical interpretation based on the ideas of dispersive wave propagation and group velocity. Group velocity effects in finite-difference modeling have been surveyed by me in [9] and by Vichnevetsky and Bowles in [13]; others who have been interested in these matters include Matsuno, Grotjahn, and O'Brien in meteorology; Alfold, Bamberger, and Martineau-Nicoletis in geophysics; Kentzer, Giles, and Thompkins in aerodynamics; and Hedstrom and Chin in theoretical numerical analysis. I have described a group velocity interpretation of the one-boundary stability problem in [10], showing in particular how the GKS "perturbation test" for unstable "generalized eigensolutions" is equivalent to a test of the sign of a group velocity. In [11] this approach is made rigorous, and various theorems on unstable growth rates are obtained. In [12] I have extended these ideas to problems with two or more boundaries or internal interfaces, where stability depends on what happens when wave packets reflect back and forth. The latter work was motivated in part by ideas of Kreiss

(see e.g. Sec. 7 of [4]), of Beam, Warming, and Yee [1], and of Giles and Thompkins [2].

There is an analogous theory for p.d.e.'s rather than difference approximations. Again, wave radiation from the boundary is a general mechanism of ill-posedness. See Kreiss [6] for the basic theory, and the new survey by Higdon [5] for the wave interpretation. The difference is that for p.d.e.'s, nontrivial cases of ill-posedness do not arise unless the domain contains two or more space dimensions.

The purpose of this paper is to survey these results relating stability and wave propagation by means of an extended example. With the aid of many illustrations we will see exactly how waves can get amplified by reflection at boundaries and how this can lead to instability.

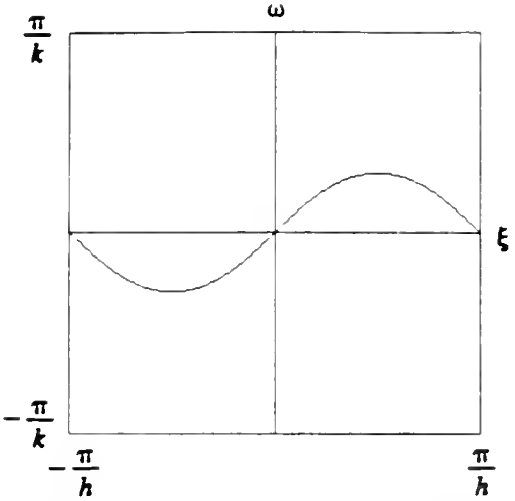

Figure 1.1. Dispersion relation for Crank-Nicolson with $\lambda = 1$.

Now that the dispersion function is known we can synthesize v^n as follows:

$$v_j^n = \frac{1}{2\pi} \int_{-\pi/h}^{\pi/h} e^{i(\omega(\xi)t+\xi x)} \hat{v}^0(\xi)\,d\xi, \quad x = jh, \quad t = nk. \tag{1.5}$$

Armed with this equation we could duplicate the behavior of CN by computing Fourier integrals. There is little profit in that, but what (1.5) does offer is the prospect of approximate evaluation by a stationary phase argument. For observe that the exponential term introduces an oscillatory behavior that will make the integrand tend to cancel to zero if $\omega(\xi)$ and $\hat{v}^0(\xi)$ are smooth. The exception is that at values of ξ satisfying

$$\frac{d}{d\xi}(\omega(\xi)t + \xi x) = 0, \quad \text{i.e.} \quad \frac{d\omega(\xi)}{d\xi} = -\frac{x}{t},$$

there is no oscillation and no cancellation. In other words, most of the energy associated with wave number ξ travels approximately at the *group velocity*

$$C = -\frac{d\omega}{d\xi}. \tag{1.6}$$

Of course this argument is vague, but it can be made precise in various ways; see for example Lemma 5.1 of [11].

Thus wave energy travels at a velocity given by the negative of the slope of the dispersion relation. For CN we can differentiate (1.4) implicitly to obtain

$$C = -\cos\xi h \cos^2\frac{\omega k}{2}. \tag{1.7}$$

Eliminating ω by means of (1.4′), or differentiating (1.4′) directly, converts this to the functional form

$$C(\xi) = \frac{-\cos\xi h}{1 + \frac{\lambda^2}{4}\sin^2\xi h}. \tag{1.7'}$$

This function is plotted in Fig. 1.2. One sees that for well-resolved waves – i.e. $\xi h << 0$, or many points per wavelength – energy travels at velocity -1, as it should according to the p.d.e. $u_t = u_x$. Less well resolved waves have lower speeds (less negative velocities), and it is this fact that gives rise to familiar oscillations around discontinuities. At the extreme, the sawtoothed (or *parasitic*) wave $v_j^n = (-1)^j$, i.e. $\xi h = \pm\pi$, has group velocity $+1$, so energy in this mode travels in the physically wrong direction.

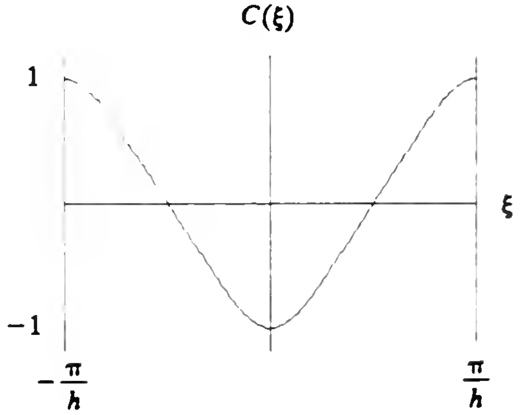

Figure 1.2. Group velocity.

Let us confirm this last prediction by an experiment. Fig. 1.3 shows the evolution under CN with $h = .01$ and $\lambda = 1$ of an initial signal

$$v_j^n = [1+(-1)^j]\, e^{-400(x-.5)^2}$$

on the interval [0,1]. This "rectified Gaussian", shown in Fig. 1.3a, contains equal amounts of energy at $\xi h = 0$ and at $\xi h = \pm\pi$. Figures 1.3b and 1.3c show the wave forms

at times .2 and .4. As predicted, the two wave components have separated and traveled in opposite directions. This backwards motion of the parasitic wave component is of course a purely numerical effect. For further examples see [9] and [13].

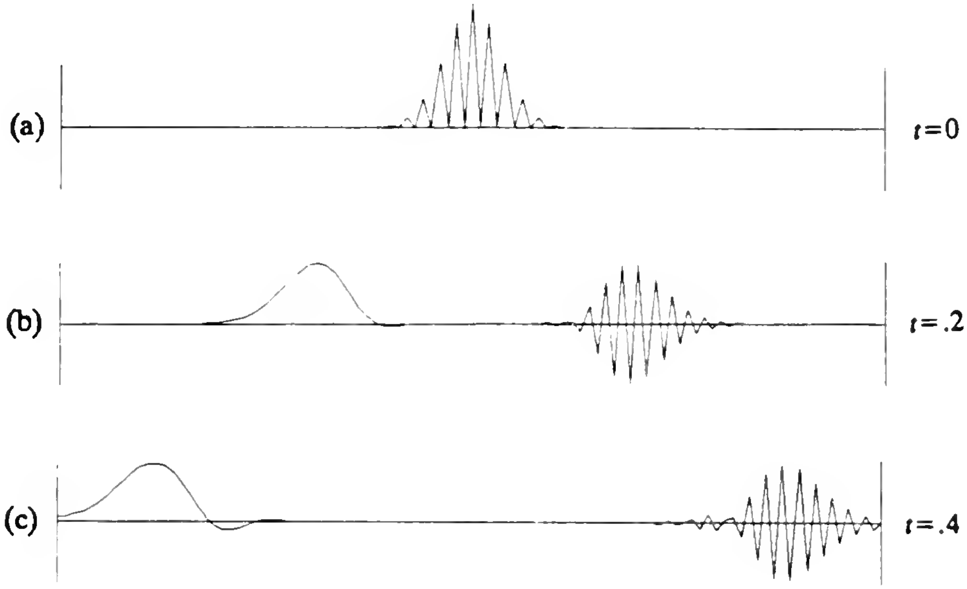

Figure 1.3. Propagation of energy at group velocities $C=\pm 1$.

In analyzing the behavior of an arbitrary difference model, a useful question to ask is: given a frequency ω_0, what associated wave numbers ξ are admitted by the dispersion relation, and how do the corresponding waves $\exp(i(\omega_0 t+\xi x))$ propagate? To get the answer for CN, imagine drawing a horizontal line at height ω_0 in Fig. 1.1. Assuming ω_0 is small enough, it will intersect the dispersion curve at two values ξ_1 and ξ_2. Of the two corresponding sine waves, one has $C\le 0$ and one has $C\ge 0$. For simplicity, from now on we will write η for the wave number corresponding to $C\le 0$ and ξ for the other one. By (1.4), ξ and η are related under CN by

$$\xi = \frac{\pi}{h}-\eta \qquad \begin{array}{l}\xi\text{: rightgoing}\\ \eta\text{: leftgoing}\end{array} \quad . \tag{1.8}$$

The same relationship holds for any difference model, such as leap frog or backwards Euler, whose spatial discretization consists of the usual second-order centered difference.

As a more complicated example, suppose we had a nondissipative difference formula with the dispersion function plotted in Fig. 1.4. (An arbitrary continuous dispersion function defines a bounded operator $v^n \mapsto v^{n+1}$ in l^2, a *Fourier multiplier*, but this operator can be realized by finite differences only when the function is the solution of a trigonometric polynomial equation in ω and ξ.) According to the figure, there are four wave numbers ξ_ν associated with the frequency ω_1. ξ_1 and ξ_3 correspond to leftgoing waves, and ξ_2 and ξ_4 to rightgoing waves.

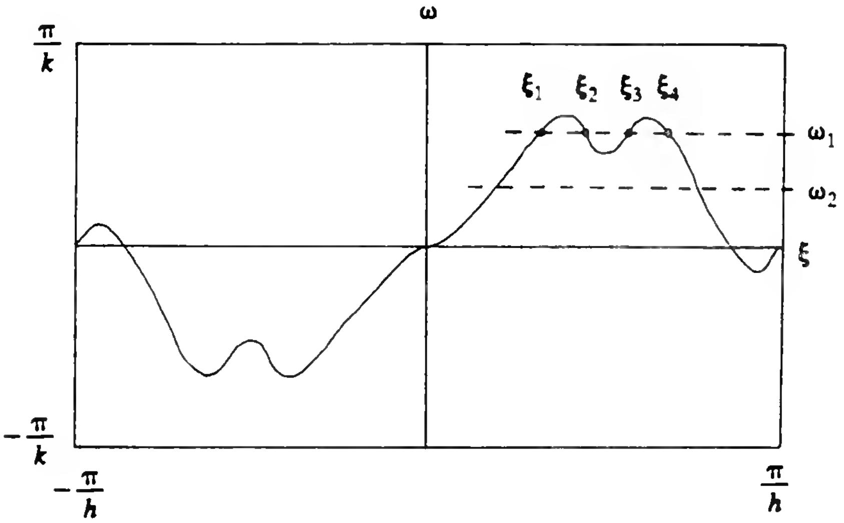

Figure 1.4. Dispersion relation for an unknown difference formula.

On the face of it the situation looks different at frequency ω_2 -- there is only one wave propagating in each direction. However in fact, the missing two wave numbers still exist, but they have become complex. One has negative imaginary part, and corresponds to a leftgoing evanescent wave that does not carry energy; the other has positive imaginary part and is evanescent and rightgoing.

Actually, as far as one can tell from Fig. 1.4, evanescent modes may exist at frequency ω_1 too. This depends on the size of the stencil of the difference formula. The general situation is this: for a scalar difference formula with stencil extending l points to the left of center and r points to the right, the dispersion relation is a trigonometric polynomial in ξ of order $l+r$, which for each ω has $l+r$ complex roots ξ that break down into

exactly r "leftgoing" and l "rightgoing" linearly independent wave modes. Here we say that a wave $\exp(i(\omega t+\xi x))$ with $\mathrm{Im}\,\omega=0$ (or more generally $\mathrm{Im}\,\omega\leq 0$) is *rightgoing* if either

(1) $\mathrm{Im}\,\xi=0$ and $C(\xi,\omega)\geq 0$

or

(2) $\mathrm{Im}\,\xi>0$.

A *leftgoing* wave is defined with the directions of the inequalities in (1) and (2) reversed. These definitions and their consequences are studied in detail in [11].

Thus the general solution of the form $v_j^n = e^{i\omega t}\phi_j$ to an arbitrary scalar finite difference formula can be written

$$v_j^n = \underbrace{e^{i\omega t}\sum_{\nu=1}^{l}\alpha_\nu e^{i\xi_\nu x}}_{(rightgoing)} + \underbrace{e^{i\omega t}\sum_{\nu=1}^{r}\beta_\nu e^{i\eta_\nu x}}_{(leftgoing)}, \qquad x=jh, \quad t=nk. \tag{1.9}$$

For convenience I have relabeled $\alpha_{l+1},\ldots,\alpha_{l+r}$ by $\beta_1,\ldots,\beta_r$, and $\xi_{l+1},\ldots,\xi_{l+r}$ by $\eta_1,\ldots,\eta_r$.

2. One boundary: reflection coefficients

What if we now let more time elapse in Fig. 1.3, so that the waves hit the boundaries at $x=\pm 1$? The result will of course depend on the boundary conditions there.

The general principle for analyzing such problems is to look for solutions containing only a single frequency ω_0. Different frequencies can be superposed later. If a wave $\exp(i(\omega_0 t+\xi_0 x))$ hits a boundary, then the reflected result after the initial transient has died away will be a linear combination of waves $\sum \alpha_\nu \exp(i\omega_0 t+\xi_\nu x))$ with the same frequency ω_0 but with various new wave numbers ξ_ν. In general the wave numbers in the reflected waves will be all of those fulfilling the following two conditions:

(1) ω_0, ξ_ν satisfy the dispersion relation.

(2) The wave $\exp(i(\omega_0 t+\xi_\nu x))$ propagates away from the boundary into the interior (the *radiation condition).* This means that any wave reflected at a lefthand boundary must be rightgoing, and any wave reflected at a righthand boundary must be leftgoing.

Neither of these statements mentions the boundary conditions. Those do not affect the set of reflected waves, just the coefficients α_ν.

To compute numerical reflection coefficients one simply inserts the wave (1.9) into the numerical boundary conditions. For a general formulation consider a lefthand boundary at $x=j=0$, and let the numerical boundary conditions there consist of l linear homogeneous equations giving $v_0^{n+1}, \ldots, v_{l-1}^{n+1}$ as linear combinations of other values v_j^n. Insertion of (1.9) yields a linear *reflection equation*

$$E(\omega)\alpha = D(\omega)\beta \tag{2.1}$$

relating leftgoing and rightgoing wave coefficients. Here E and D are matrices of dimensions $l\times l$ and $l\times r$, respectively. If $E(\omega)$ is nonsingular we can solve for the rightgoing wave coefficients to get

$$\alpha = A(\omega)\beta = [E(\omega)]^{-1}D(\omega)\beta. \tag{2.2}$$

$A(\omega)$ is called the *reflection matrix*. Compare [4], eq. (10.2).

Figure 2.1 shows what happens when the integration of Fig. 1.3 is carried to $t>1/2$ with the following conditions at the boundaries:

$$v_0^{n+1} = v_1^{n+1}, \tag{2.3a}$$

$$v_J^{n+1} = 0. \tag{2.4a}$$

Here $J=1/h$ is the index of the grid point at the boundary $x=1$. Figs. 2.1a and 2.1b show the configuration at time $t=.6$ and $t=.8$.

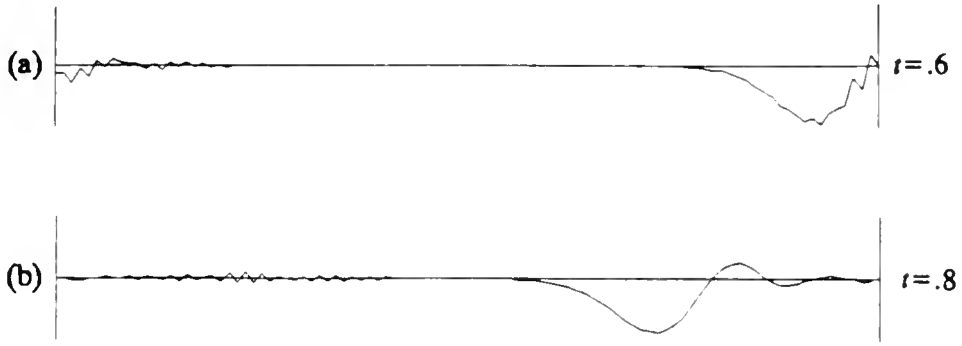

Figure 2.1. Continuation of Fig. 1.3 showing reflection at boundaries.

Clearly the leftgoing pulse with $\eta=0$ has generated a rightgoing reflected wave with $\xi=\pi/h$ at very small amplitude. The rightgoing pulse with $\xi=\pi/h$ has generated a considerably larger reflection with $\eta=0$. Let us predict these reflected amplitudes after the fact.

First we compute the reflection coefficient for (2.3a). In the present case (1.8) implies that (1.9) reduces to

$$v_j^n = [\alpha e^{i\xi x}+\beta e^{i\eta x}]e^{i\omega t} = [(-1)^j\alpha e^{-i\eta x}+\beta e^{i\eta x}]e^{i\omega t}, \quad x=jh,\ t=nk. \tag{2.5}$$

For simplicity in such computations it is convenient to introduce the abbreviations

$$\kappa = e^{i\xi h}, \quad \mu = e^{i\eta h}, \quad z = e^{i\omega k}. \tag{2.6}$$

Then (2.5) becomes

$$v_j^n = (\alpha\kappa^j+\beta\mu^j)z^n. \tag{2.7}$$

For CN (1.8) becomes $\kappa=-1/\mu$. Inserting (2.7) in (2.3a) gives

$$\alpha+\beta = (\alpha\kappa+\beta\mu) = -\alpha/\mu+\beta\mu.$$

In the form of (2.1) this is

$$(1+\frac{1}{\mu})\alpha = (\mu-1)\beta, \tag{2.3b}$$

that is,

$$\frac{\alpha}{\beta} = \mu\frac{\mu-1}{\mu+1} = ie^{i\eta h}\tan\frac{\eta h}{2}. \tag{2.3c}$$

For $\eta \approx 0$, as in the present experiment, we get $\alpha/\beta \approx 0$, and this explains the very small amplitude of the pulse reflected from the lefthand boundary in Fig. 2.1.

Now the analogous computation for (2.4a). Inserting (2.7) gives

$$\kappa^J \alpha = -\mu^J \beta, \tag{2.4b}$$

that is,

$$\frac{\alpha}{\beta} = -(-\mu^2)^J = (-1)^{J+1} e^{2Ji\eta}. \tag{2.4c}$$

Thus the amplitude of the reflected wave should be equal and opposite to that of the incident wave, regardless of η. Fig. 2.1 confirms this nicely.

Let us return to the lefthand boundary and consider some alternative boundary conditions. Suppose we replace (2.3a) by

$$v_0^{n+1} = v_1^n. \tag{2.8a}$$

Then insertion of (2.7) leads to

$$(z + \frac{1}{\mu})\alpha = (-z + \mu)\beta, \tag{2.8b}$$

or

$$\frac{\alpha}{\beta} = \mu \frac{\mu - z}{1 + \mu z} = i\, e^{i\eta h} \sin \frac{\eta h - \omega k}{2} \Big/ \cos \frac{\eta h + \omega k}{2}. \tag{2.8c}$$

Again this predicts a near-zero reflected amplitude for $\eta \approx 0 \approx \omega$. On the other hand suppose we impose

$$v_0^{n+1} = v_2^{n+1}. \tag{2.9a}$$

The reflection equation is then

$$(1 - 1/\mu^2)\alpha = (\mu^2 - 1)\beta. \tag{2.9b}$$

This implies

$$\frac{\alpha}{\beta} = \mu^2 = e^{2i\eta h} \tag{2.9c}$$

much as in (2.4c), at least for $\eta \neq 0$. At $\eta = 0$ (2.9b) has the form $0\alpha = 0\beta$, so it is not solvable except in a limiting sense.

Figure 2.2 plots results of experiments with boundary conditions (2.8a) and (2.9a). Fig 2.2a shows the initial condition, a leftgoing wave with $\eta = 0$ on a mesh with $h = .01$ for $[0,1]$, and Figs. 2.2b and 2.2c show the results at $t = 1$ under (2.8a) and (2.9a),

respectively. The predicted reflection coefficients 0 and 1 are clearly in evidence. In fact no reflected energy at all is visible in Fig. 2.2a; this is because with $\lambda=1$, i.e. $h=k$, (2.8c) is identically zero.

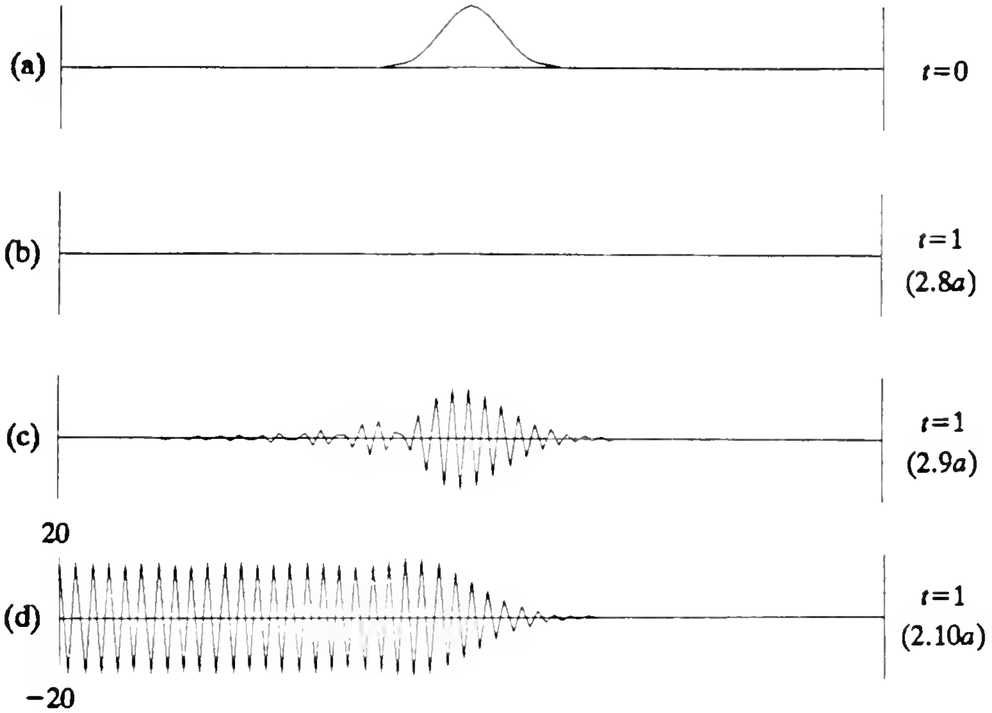

Figure 2.2. Effect of various lefthand boundary conditions.

Figure 2.2d shows the response of CN to the same initial data with a more contrived boundary condition:

$$v_0^{n+1} = -v_1^{n+1} + v_2^{n+1} + v_3^{n+1}. \tag{2.10a}$$

This time a marked instability is evident (note the vertical scale). To see why, compute the reflection equation

$$[1+\kappa-\kappa^2-\kappa^3]\alpha = -[1+\mu-\mu^2-\mu^3]\beta,$$

which can be simplified to

$$(1+\mu)(1-\mu)^2\alpha = -\mu^3(1+\mu)^2(1-\mu)\beta, \tag{2.10b}$$

that is,

$$\frac{\alpha}{\beta} = -\mu^3\frac{1+\mu}{1-\mu} = ie^{3i\eta h}\cot\frac{\eta h}{2}. \tag{2.10c}$$

At $\eta=0$, this reflection coefficient is *infinite*.

The existence of a frequency ω at which the reflection coefficient at a boundary is infinite implies that a finite-difference model is unstable. In [11] it is shown that under reasonable assumptions, such a model potentially amplifies initial data in the l^2 norm at a rate at least proportional to the time step number n. Obviously this is an unstable situation, since as h and k are decreased, the index n corresponding to a fixed time t increases to ∞.

The presence of an infinite reflection coefficient is a stronger condition than "GKS-instability," a name sometimes given to instability according to Defn. 3.3 of [4]. In fact a difference model is GKS-unstable if and only if the matrix $E(\omega)$ in (2.1) is singular for some ω with $\mathrm{Im}\,\omega\leq 0$, i.e. $|z|\geq 1$ (Thm. 1a of [11]). For scalar problems with three-point stencils this amounts to the condition that the coefficient of α on the left side of a reflection equation such as (2.3b), (2.4b), (2.8b), (2.9b), or (2.10b) is 0 for some ω. Thus, for example, the boundary condition (2.9a) is GKS-unstable for CN, since the lefthand side of (2.9b) is zero at $\mu=z=1$, even though no apparent catastrophe occurred in Fig. 2.2c. In such situations the reflection coefficient remains finite if it happens that the righthand side of the reflection equation has a zero at the same value of ω of at least as high an order. When this occurs, it is shown in [11] that unstable growth of initial data in the l^2 norm need proceed no faster than in proportion to $\sqrt{n}$.

To summarize, there are at least three distinct circumstances that may obtain at the boundary:

(1) nonsingular refl. eq., finite refl. coeff.: stable ($||v||=O(1)$);

(2) singular refl. eq., finite refl. coeff.: weakly unstable ($||v||=O(\sqrt{n})$);

(3) singular refl. eq., infinite refl. coeff.: unstable ($||v||=O(n)$).

3. Two boundaries: reflection back and forth

What if we let even more time elapse in Figs. 1.3 and 2.1? The answer is simple: new reflections will occur as the two wave packets bounce back and forth between $x=0$ and $x=1$. Each time a rightgoing wave packet with $\xi \approx \pi/h$ hits $x=1$, it will reflect as a leftgoing wave packet with $\eta \approx 0$ having essentially the same amplitude. But each time a leftgoing wave hits $x=0$, it will reflect as a rightgoing wave of greatly diminished amplitude. The total energy in [0,1] will consequently decay rapidly to near 0. The reason one can only say "near" is that a certain portion of the energy will have $\xi \approx \pi/2h$, and since $C=0$ at this wave number, this portion tends to stay in a fixed position and never hit the boundaries.

Figs. 3.1a and 3.1b confirm this prediction by showing the numerical solutions at $t=2$ and $t=4$. At $t=2$ the signal that remains is very weak, and at $t=4$ it is somewhat weaker.

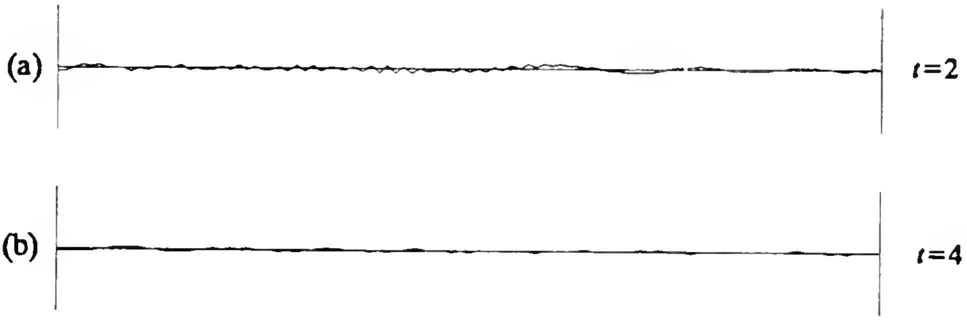

Figure 3.1. Further continuation of Figs. 1.3 and 2.1.

Suppose, more generally, we set up the CN model on an interval $[0,L]$ with some pair of stable boundary conditions at $x=0$ and $x=L$ for which the reflection coefficient functions are $A_1(\omega)$ and $A_2(\omega)$, respectively. If v^0 is a wave packet with frequency ω, then as t increases this packet will reflect back and forth, undergoing amplification by $|A_1|$ or $|A_2|$ each time it hits a boundary. Let $C(\omega)$ denote the group speed $|C(\xi,\omega)| = |C(\eta,\omega)|$. Then the travel time for a complete circuit involving a reflection at each boundary will be

$$T(\omega) = \frac{2L}{C(\omega)}. \tag{3.1}$$

After such a circuit the amplitude will have increased by a factor

$$\alpha(\omega) = |A_1(\omega)A_2(\omega)|. \tag{3.2}$$

Combining these formulas, we reach the following conclusion: as $t \to \infty$, energy associated with frequency ω grows approximately at the rate

$$\frac{\|v(t)\|}{\|v(0)\|} \approx \alpha(\omega)^{t/T(\omega)} = \alpha(\omega)^{tC(\omega)/2L}. \tag{3.3}$$

For $\alpha > 1$ this equation predicts exponential growth, and for $\alpha < 1$, exponential decay.

On the basis of this analysis one can now make some very interesting observations about stability and convergence. The following ideas are spelled out in detail in [12].

The first observation is, *stability does not preclude exponential growth in time.* We have seen in the last section that stability for a single boundary implies $A < \infty$, but not $A \leq 1$. Thus it is easily possible for a model composed of two individually stable boundaries to generate growth of truncation errors at a rate exp(const$t$). One might think that this reveals that the concatenation of two stable boundaries is in general unstable. But in fact, exponential growth does not imply instability in the usual Lax-Richtmyer sense, and it will not prevent convergence. The reason is that the growth factor for any fixed t does not get larger as $h,k \to 0$, whereas the truncation errors that the factor multiplies get smaller (by consistency).

These conclusions are already known. In fact Thm. 5.4 of [4] asserts that in general, the concatenation of two GKS-stable difference schemes is always GKS-stable, while Sec. 7 of [4] investigates the conditions under which exponential growth in t will occur for a particular stable 2×2 example. What is new here is the interpretation by reflection coefficients. This interpretation also helps to clear up a misconception. Some people have thought that although exponential growth can occur for finite h and k, it must vanish as $h,k \to 0$. But the study of reflecting wave packets gives no reason to expect such good fortune, and an example in [12] proves that indeed it is not to be expected. To be sure of eliminating growth by refining the mesh, one needs a difference formula that is suitably dissipative [3].

There is a reason why exponential growth in t may be a problem: in practice, time dependent finite difference models are often used (especially in aerodynamics) to compute approximate solutions for the steady state $t \to \infty$. Obviously growth of errors at a rate $e^{\text{const}t}$ will make such a procedure fail. With this in mind, Beam, Warming, and Yee [1] have defined a difference model to be *P-stable* if it is GKS-stable, and in addition, it admits no

exponentially growing modes. In this language the above observation becomes: stability does not imply P-stability.

Our second observation now comes as the natural complement to the first: *having reflection coefficients bounded by* 1 *does preclude exponential growth in time.* For in (3.3) we see that if $\alpha(\omega)\leq 1$ for every ω, then no frequency exists that can experience repeated amplification by reflection. This argument can be made rigorous, and Prop. 11 of [12] states: if $\alpha(\omega)\leq 1$ for every ω, a difference model is P-stable.

For a third and final observation, let us turn to the case in which one or both boundaries is individually unstable. Then we find, *a mildly unstable boundary with an infinite reflection coefficient may become catastrophically unstable when a second boundary is introduced.* For consider a boundary condition which has $A(\omega_0)=\infty$ for some ω_0. If a wave packet at frequency ω_0 hits this boundary, it will be amplified by a large factor (typically $O(N)$, where N is the width of the packet in grid points). For a single boundary, this is a one-time-only event, as in Fig. 2.2d. But when there are two boundaries, the reflected wave may reflect at the other boundary, then return to be amplified again, and so on. For boundaries separated by N grid points one gets growth potentially at a very rapid rate

$$\frac{||v(t)||}{||v(0)||}\approx N^{\mathrm{const}\,t} = N^{\mathrm{const}\,nk}.$$

This instability is a far cry from the growth proportional to n mentioned in the last section, and it renders the difference model totally useless.

This phenomenon of catastrophic two-boundary interactions was first noted long ago by Kreiss. The advantage of the present point of view is that it makes it clear that the problem is associated not with all unstable boundaries, but only with those having infinite reflection coefficients. Unstable boundary conditions with finite reflection coefficients typically exhibit only weak instability even when other boundaries are present. Of course, sometimes weak instabilities may be more dangerous than strong ones, since they can more easily go undetected.

Our final numerical experiment, summarized in Fig. 3.2, illustrates the difference in two-boundary behavior between unstable boundary conditions with finite and infinite reflection coefficients. Fig. 3.2a shows the initial data, a uniformly distributed random signal on the usual CN mesh on [0,1]. At $x=1$ the boundary condition is (2.4a). First an integration was performed with the boundary condition (2.9a) at $x=0$, which is unstable but by (2.9c) has a finite reflection coefficient. In this process nothing dramatic occurs, no matter how large t is. Fig. 3.2b shows the result at $t=10$, and it looks qualitatively

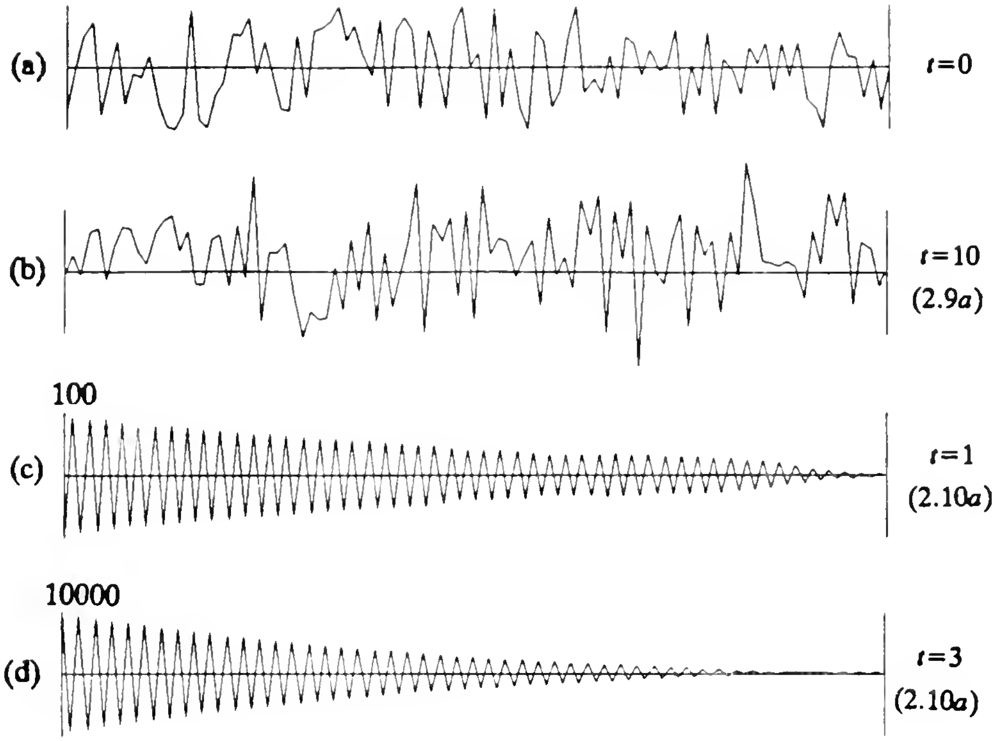

Figure 3.2. Two-boundary interactions

much like the initial data. Of course this does not imply that this model will give accurate answers to physical problems, but it does reveal that GKS-instability of a boundary condition does not by itself lead to explosive two-boundary interactions.

In contrast, Figs. 3.2c-d show results obtained with boundary condition (2.10a), which has an infinite reflection coefficient. The plots show times $t=1,3$. Note the vertical scales.

In summary, for two-boundary problems one has the following possibilities:

(1) stable b.c.'s, $0 \leq \alpha \leq 1$: stable and P-stable ($\|v\| = O(1)$)

(2) stable b.c.'s, $1 < \alpha < \infty$: stable but P-unstable ($\|v\| = O(e^{\mathrm{cons}u})$)

(3) unstable b.c.'s, $0 \leq \alpha < \infty$: weakly unstable ($\|v\| = O(\sqrt{n})$)

(4) unstable b.c.'s, $\alpha = \infty$: catastrophically unstable ($\|v\| = O(N^{\mathrm{cons}u})$)

Before closing, a word must be said about dissipation. I have presented a picture in which numerical waves bounce back and forth between boundaries, with changes of amplitude occurring at each reflection but not during the transit in between. Under a dissipative difference formula, however, any wave with $\xi \neq 0$ decays as it travels. The result is that the two-boundary interactions I have spoken of rarely take place, so that in practice, the behavior of a dissipative two-boundary model is not much different from what the individual boundaries would suggest. The exceptions occur when the dissipation is very weak, as in the problems with large mesh ratios considered in [1]; or when the number of grid points between boundaries is very small, as in certain cases discussed in Sec. 2 of [12].

For an overall summary, one may say that difference models for hyperbolic partial differential equations exhibit three important physical processes: propagation, reflection, and dissipation of waves. In general the waves involved are numerical objects with no physical meaning, but they are still important to stability. An exact mathematical analysis of a finite difference model is usually too difficult to be practical, but even for complicated models one can often gain insight fairly easily by considering these physical processes.

References

[1] R. Beam, R. Warming, and H. Yee, Stability analysis for numerical boundary conditions and implicit difference approximations of hyperbolic equations, *Proc. NASA Symp. on Numerical Boundary Procedures,* 1981, 199-207.

[2] M. Giles and W. Thompkins, Jr., Asymptotic analysis of numerical wave propagation in finite difference equations, Gas Turbine and Plasma Phys. Lab. Rep. 171, Mass. Inst. Tech., 1983.

[3] B. Gustafsson, The choice of numerical boundary conditions for hyperbolic systems, *Proc. NASA Symp. on Numerical Boundary Procedures,* 1981, 209-225.

[4] B. Gustafsson, H.-O. Kreiss, and A. Sundström, Stability theory of difference approximations for initial boundary value problems. II, *Math. Comp. 26* (1972), 649-686.

[5] R. Higdon, Initial-boundary value problems for linear hyperbolic systems, *SIAM Review,* to appear.

[6] H.-O. Kreiss, Initial boundary value problems for hyperbolic systems, *Comm. Pure Appl. Math. 23* (1970), 277-298.

[7] S. Osher, Systems of difference equations with general homogeneous boundary conditions, *Trans. Amer. Math. Soc. 137* (1969), 177-201.

[8] R. Richtmyer and K. Morton, *Difference Methods for Initial-Value Problems,* Wiley-Interscience, 1967.

[9] L. N. Trefethen, Group velocity in finite difference schemes, *SIAM Review 24* (1982), 113-136.

[10] L. N. Trefethen, Group velocity interpretation of the stability theory of Gustafsson, Kreiss, and Sundström, *J. Comp. Phys. 49* (1983), 199-217.

[11] L. N. Trefethen, Instability of finite difference models for hyperbolic initial boundary value problems, *Comm. Pure Appl. Math.,* to appear.

[12] L. N. Trefethen, Stability of finite difference models containing two boundaries or interfaces, to appear.

[13] R. Vichnevetsky and J. Bowles, *Fourier Analysis of Numerical Approximations of Hyperbolic Equations,* SIAM, 1982.

This book may be kept

FOURTEEN DAYS

A fine will be charged for each day the book is kept overtime.

GAYLORD 142

PRINTED IN U.S.A.

NYU c.1
Comp. Sci. Dept.
TR-97 Trefethen
Stability of hyperbolic
finite-difference models.

c.1
NYU
Comp. Sci. Dept.
TR-97 Trefethen
AUTHOR
Stability of hyperbolic
TITLE
finite-difference models.

DATE DUE	BORROWER'S NAME

LIBRARY
N.Y.U. Courant Institute of
Mathematical Sciences
251 Mercer St.
New York, N. Y. 10012